Published online 26 August 2022

Nucleic Acids Research, 2022, Vol. 50, No. 16 ***9195–9211***
https://doi.org/10.1093/nar/gkac707

Enhancer looping protein LDB1 regulates hepatocyte gene expression by cooperating with liver transcription factors

Guoyou Liu [1,*], Lei Wang[2], Jürgen Wess [2] and Ann Dean [1,*]

[1]Laboratory of Cellular and Developmental Biology, National Institute of Diabetes and Digestive and Kidney Diseases, National Institutes of Health, Bethesda, MD 20892, USA and [2]Laboratory of Bioorganic Chemistry, National Institute of Diabetes and Digestive and Kidney Diseases, National Institutes of Health, Bethesda, MD 20892, USA

Received June 28, 2022; Editorial Decision July 23, 2022; Accepted August 22, 2022

ABSTRACT

Enhancers establish proximity with distant target genes to regulate temporospatial gene expression and specify cell identity. Lim domain binding protein 1 (LDB1) is a conserved and widely expressed protein that functions as an enhancer looping factor. Previous studies in erythroid cells and neuronal cells showed that LDB1 forms protein complexes with different transcription factors to regulate cell-specific gene expression. Here, we show that LDB1 regulates expression of liver genes by occupying enhancer elements and cooperating with hepatic transcription factors HNF4A, FOXA1, TCF7 and GATA4. Using the glucose transporter *SLC2A2* gene, encoding GLUT2, as an example, we find that LDB1 regulates gene expression by mediating enhancer–promoter interactions. *In vivo*, we find that LDB1 deficiency in primary mouse hepatocytes dysregulates metabolic gene expression and changes the enhancer landscape. Conditional deletion of LDB1 in adult mouse liver induces glucose intolerance. However, *Ldb1* knockout hepatocytes show improved liver pathology under high-fat diet conditions associated with increased expression of genes related to liver fatty acid metabolic processes. Thus, LDB1 is linked to liver metabolic functions under normal and obesogenic conditions.

INTRODUCTION

Enhancers are gene regulatory elements typically residing at considerable genomic distances from their target genes. The long-distance interaction between enhancers and genes occurs predominately within topologically associating domains (TADs). TADs are self-interacting regions of chromatin up to 1 Mb in size bordered by convergent CTCF binding sites (1–3). This organization is thought to favor enhancer interaction with appropriate target genes and restrict interaction with nontarget genes. In addition, lineage-specific protein factors bind at promoters and enhancers and contribute to the specificity with which these contacts determine unique transcriptomes in diverse cell types during development and differentiation (4,5). A large fraction of disease-associated genomic variants, including those associated with obesity and type 2 diabetes, reside in regulatory regions of the genome that are likely to be enhancers (6,7).

Lim domain binding protein 1 (LDB1) is a highly conserved and ubiquitously expressed enhancer–promoter looping factor that is critical for several developmental pathways in diverse invertebrate and vertebrate organisms (8). Deletion of *Ldb1* in the mouse causes embryonic lethality at around E8.5 with numerous developmental defects in body pattern formation and abnormalities in cardiogenesis, neurogenesis and hematopoiesis (9). To be able to bind to chromatin, the LIM-interacting domain in the C-terminus of LDB1 binds to LIM homeodomain proteins or to LIM-only proteins that require additional partners to bind DNA. Enhancer binding complexes of LDB1 with specific nuclear LIM domain proteins are implicated in numerous developmental systems (8).

The liver is a critical organ for detoxification and metabolism and contributes to maintenance of normal blood glucose levels. It has been reported that knockout (KO) of *Ldb1* in hepatocytes disrupts normal gene expression and promotes diethylnitrosamine-induced liver cancer in mice (10). However, how LDB1 normally functions in the liver is unknown. Here, we show by RNA sequencing (RNA-seq) that genes dysregulated upon LDB1 loss in the human HepG2 hepatoma cell line are enriched for liver metabolic pathways. ChIP sequencing (ChIP-seq) re-

*To whom correspondence should be addressed. Tel: +1 301 496 6068; Email: ann.dean@nih.gov
Correspondence may also be addressed to Guoyou Liu. Tel: +1 301 435 9396; Email: guoyou.liu@nih.gov
Present address: Lei Wang, Department of Food and Nutritional Hygiene, School of Public Health, Capital Medical University, No. 10, Xitoutiao, You An Men Wai, Beijing 100069, China.

vealed that LDB1 binds primarily to enhancers at sites that overlap with core liver transcription factors. KO of LDB1 significantly decreased expression of the major glucose transporter gene *SLC2A2*. Mechanistically, LDB1 mediated chromatin interactions between the gene promoter and its enhancers in an LDB1-dependent fashion and KO of LDB1 decreased liver transcription factor binding at these regulatory elements. *In vivo* studies showed that conditional KO of LDB1 in mouse hepatocytes (hep-*Ldb1*^{cKO}) impacted H3K27ac modification in the genome and dysregulated expression of hundreds of genes enriched in metabolic pathways such as fatty acid metabolic processes. When hep-*Ldb1*^{cKO} mice were maintained on a high-fat diet (HFD), the pathological liver steatosis that typically develops in obese mice was greatly attenuated. Thus, LDB1 organizes chromatin interactions and regulates metabolic gene expression in hepatocytes and maintains essential metabolic functions of the liver.

MATERIALS AND METHODS

Mouse model

All animal studies were approved by the NIDDK/NIH Animal Care and Use Committee. Mice were housed in a clean conventional vivarium at ∼22°C, with a 12:12 h dark–light cycle (lights on at 06:00), and ad libitum access to water and chow (LabDiet, Advanced Protocol 5V0T, 12.5% kcal from fat) or HFD (89067-469, 60% kcal fat, VWR). *Ldb1* flox mice (11) and Albumin-Cre mice (003574, The Jackson Laboratory) were mated to obtain control mice (*Ldb1*$^{flox/flox}$) and liver-specific Ldb1 KO mice (*Ldb1*$^{flox/flox}$;*Alb-Cre*$^{+/-}$) on a C57Bl6 background. Only male littermates were used for experiments to control for the effects of sex on metabolic studies. All regular chow (RC) experiments were performed in 7–12-week-old mice. When indicated, 8-week-old mice started to consume an HFD for 11–16 weeks.

Cell culture and transfection

HepG2 cells (HB-8065, ATCC) were cultured according to instructions. To generate LDB1 KO HepG2 clones, pSpCas9-2A-GFP plasmid (Addgene, Plasmid #4813) containing a guide RNA targeting the first exon of the *LDB1* gene was electroporated into HepG2 cells (Lonza Nucleofector Kit V, VCA-1003). To generate GLUT2 E3 KO clones, two guide RNAs targeting E3 ends were electroporated into HepG2 cells. GFP-positive single cells were isolated by flow cytometry sorting and diluted and plated into 96-well plates. LDB1 KO cell clones were identified by DNA sequencing of *LDB1* gene locus and by western blotting. GLUT2 E3 KO clones were identified by PCR and DNA sequencing. To stably overexpress LDB1 in HepG2, the pMYs-IRES-Neo-LDB1 vector was used (12).

Mouse phenotyping

Body composition was measured in non-anesthetized mice by time-domain Echo MRI 3-in-1 (Echo Medical Systems, Houston, TX). Intraperitoneal glucose tolerance tests (IGTTs; 2 g/kg for RC mice, 1 g/kg for HFD mice) were performed following an overnight fast (∼13 h). Insulin tolerance tests (ITTs; Humulin R, Eli Lilly, 0.75 U/kg i.p. for RC mice, 1 U/kg for HFD mice) were performed in mice fasted for 4 h. For pyruvate tolerance tests (PTTs), mice maintained on RC were fasted overnight (∼13 h) and injected with 2 g/kg pyruvate i.p. For glucagon challenge tests (GCTs), mice were fasted for 4 h, and 16 μg/kg (for both RC and HFD mice) glucagon (Sigma, G2044) was administered i.p. In all *in vivo* assays, blood was collected from the tail vein, and blood glucose was measured with a Glucometer Contour (Bayer, Mishawaka, IN). For serum analysis, blood was collected at 09:00 from the tail vein of freely fed mice. Plasma free fatty acid (FFA; Roche Diagnostics GmbH, Mannheim, Germany), triglycerides (TGs; Pointe Scientific Inc., Canton, MI) and cholesterol (Thermo Scientific, Middletown, VA) were measured using the indicated colorimetric assays. Plasma insulin levels were measured by ELISA (Crystal Chem, Downers Grove, IL). Liver TGs were extracted from 50 mg of liver using chloroform:methanol (2:1) as described (13) and measured using Triglyceride Liquid Reagent Set (Fisher Scientific, T7532-120).

Isolation of mouse primary hepatocytes and glucose production study

Mice were anesthetized with single i.p. injection of tribromoethanol (10 μl/g of 2.5% tribromoethanol, Sigma, T48402). Subsequently, hepatocytes were isolated by a two-step collagenase perfusion method (14). After isolation, primary mouse hepatocytes were cultured in six-well plates (5×10^5 cells/well) with 10% FBS DMEM (high glucose) for ∼5 h for plating. Cells were washed twice with PBS and then incubated overnight in phenol red-free, glucose-free DMEM supplemented with gluconeogenic substrates (20 mM sodium lactate, 2 mM sodium pyruvate). Cells were washed three times with PBS. Control cells were incubated with phenol red-free, glucose-free DMEM. For glucagon stimulation, glucagon (Sigma, G2044, final concentration 10 nM) was added to phenol red-free, glucose-free DMEM supplemented with 20 mM sodium lactate and 2 mM sodium pyruvate. The same medium without glucagon was used for control purposes. For insulin stimulation, insulin (Sigma, 91077C, final concentration 100 nM) was added. Cells were incubated for 4 h. The culture medium was collected for glucose measurement (Glucose GO Assay Kit, Sigma, GAGO20-1KT), and glucose concentrations were normalized by protein amount.

RT-qPCR and RNA-seq

RNA was extracted by PureLink RNA Mini Kit (Invitrogen, 12183020), and DNA was removed by DNase digestion (Invitrogen, 12185-010). For RT-qPCR, 2 μg total RNA was reverse transcribed to cDNA by the Superscript III first-strand synthesis system (Invitrogen, 18080051). For RNA-seq, libraries were constructed from 1 μg total RNA by using the Truseq Stranded mRNA sample preparation kit (Illumina 20020493). Quality of RNA and libraries was validated by Bioanalyzer 2100. Sequencing was performed by the NIDDK Genomics Core. See Supplementary Table S1 for RT-qPCR primers.

ChIP-qPCR and ChIP-seq

ChIP-qPCR and ChIPmentation were performed as described previously (15,16). Briefly, HepG2 cells were fixed with 1% formaldehyde (Thermo, 28908) for 10 min or fixed with double cross-linking [2 mM DSG (Thermo, 20593) at room temperature for 30 min, followed by the addition of 1% formaldehyde for 10 min). A total of 10^7 cells were used for each immunoprecipitation (IP), and chromatin was sonicated to 500–1000 bp (ChIP-qPCR) or around 300 bp (ChIPmentation) using a Bioruptor. For primers used for ChIP-qPCR, see Supplementary Table S2. For antibodies used for ChIP and ChIPmentation, see Supplementary Table S3.

Immunoprecipitation

HepG2 cells were collected and washed twice with ice-cold PBS. Cells were resuspended in ice-cold lysis buffer [50 mM Tris–HCl, 150 mM NaCl, 1 mM EDTA, 1% NP40, 0.25% sodium deoxycholate, proteinase inhibitor cocktail (Sigma P8340), PMSF (Thermo Fisher, 36978)] and then incubated on ice for 30 min with occasional stirring. Cell lysates were then centrifuged at 14 000 $\times$ *g* for 15 min at 4°C. After collection of supernatants, protein concentrations were detected by a BCA kit (Thermo Fisher, 23225). Four hundred to five hundred milligrams of protein was used for each IP assay. Whole cell extract was precleared with normal IgG antibody and then aliquoted to input, IP and IgG samples. In the case of IP and IgG samples, 5 mg antibody was added and incubated at 4°C overnight. Dynabeads (Thermo Fisher, 10002D) were added and incubated for another 4 h. Beads were then washed six times with ice-cold lysis buffer. Proteins were eluted by adding LDS loading buffer (Thermo Fisher, NP0007) to the lysis buffer and incubation at 70°C for 10 min. Supernatants were collected and processed for western blotting studies. See Supplementary Table S3 for antibodies.

Chromosome conformation capture

Chromosome conformation capture (3C) was performed as described previously (17). HepG2 cells were cross-linked with 1% formaldehyde (Thermo, 28908) for 10 min at room temperature. A total of 10^7 cells were used for 3C and digested with EcoRI (BioLabs, R3101T). Relative interaction frequency between the anchor fragment and fragments of interest was analyzed by qPCR using SYBR Green Supermix (Bio-Rad, 1725124) on the 7900HT Real-Time PCR System. Interaction frequency between two fragments within the human α-tubulin gene was used for normalization between different samples. See Supplementary Table S4 for 3C primers.

Oligonucleotides

All oligos used in this study were synthesized by Integrated DNA Technologies. For other oligo sequences including gRNA, PCR and genotyping, see Supplementary Table S5.

Quantification and statistical analysis

For *in vitro* assays, three independent experiments were carried out. For *in vivo* experiments, mouse numbers are indicated in the figure legends. All data were expressed as mean ± SD. GraphPad Prism 8.0 (GraphPad Software) was used to perform the statistical analyses. For two-group comparison, *F* test was used to test equal variance first, and then two-tailed Student's *t* test for equal variance comparison and Welch's *t* test for unequal variance comparison. For multigroup comparison, two-way ANOVA followed by Bonferroni's post hoc test was used. *P* values <0.05 were considered statistically significant: $^{*}P < 0.05$, $^{**}P < 0.01$ and $^{***}P < 0.001$.

RESULTS

LDB1 regulates metabolic gene expression in HepG2 human hepatoma cells

LDB1 function has been well studied in erythroid cells and cell lines in which LDB1 is highly expressed. We found that LDB1 was also expressed in human HepG2 cells and mouse Hepa1-6 cells, although mRNA and protein levels were reduced as compared with erythroid cell lines (Supplementary Figure S1A and B). To investigate a potential role for LDB1 in liver cells, we deleted the LDB1 gene in human HepG2 cells by CRISPR/Cas9-mediated frameshift of the open reading frame (Supplementary Figure S1C). Four clones (KO-1, KO-4, KO-5 and KO-6) with reduced LDB1 mRNA and undetectable LDB1 protein expression were obtained (Supplementary Figure S1D and E). Although HepG2 is a liver hepatoma cell line, the cells display many aspects related to the regulation of hepatic metabolism that are similar to those of hepatocytes *in vivo* (18). To ask whether LDB1 loss in HepG2 cells had functional consequences, we determined glucose transport efficiency for LDB1 KO cells and for cells overexpressing LDB1 (Figure 1A, Supplementary Figure S1E). Loss of LDB1 reduced glucose uptake by HepG2 cells and LDB1 overexpression had the opposite effect, suggesting the involvement of LDB1 in liver metabolic processes.

Transcriptomic analysis was performed by RNA-seq for a representative LDB1 KO clone (KO-1) and control cells (Figure 1B). We found 490 differentially expressed genes (DEGs) in the LDB1 KO samples compared to controls ($P_{adj} < 0.1$), of which 141 genes were upregulated and 349 were downregulated. Examples of genes strongly up- or downregulated upon LDB1 loss are shown in Figure 1C. GO analysis of DEGs showed that genes downregulated by loss of LDB1 were enriched for signatures of metabolic and biosynthetic gene expression programs such as steroid metabolic process (Figure 1D). Examples of DEGs include *ALB*, encoding the major liver protein albumin, and *SLC2A2*, encoding the glucose transporter GLUT2, which plays a key role in mediating glucose uptake by the liver. Upregulated genes upon LDB1 deletion in hepatocytes were enriched for Wnt signaling pathway genes (*PYGO1*, *NKD1*, *NOTUM*, *CELSR1*), which is consistent with earlier data in embryonic liver and *in vivo* (9,10). We conclude that LDB1 regulates metabolic gene transcription programs in HepG2 hepatoma cells.

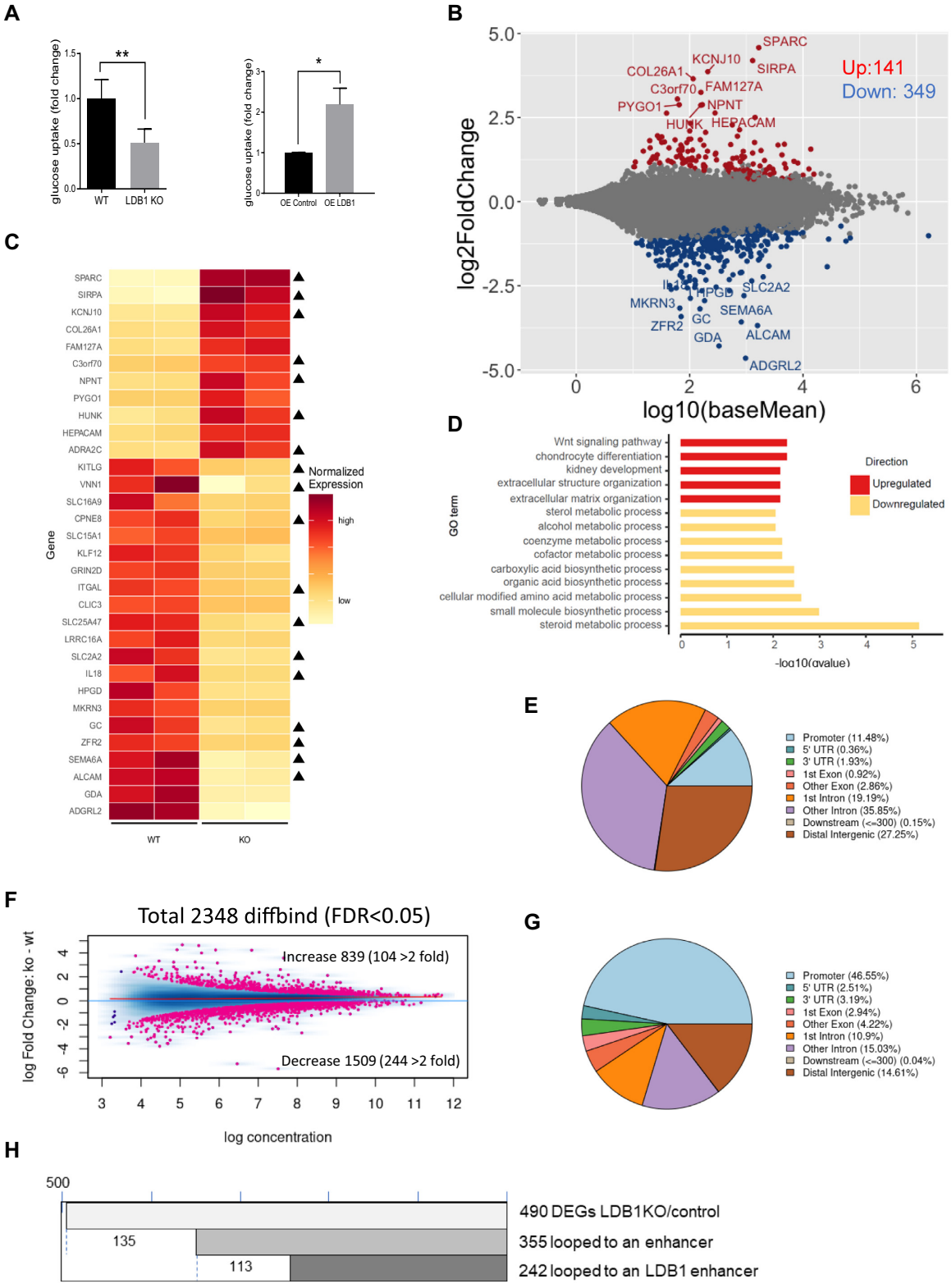

Figure 1. LDB1 regulates metabolic gene expression in HepG2 cells. (**A**) Glucose uptake measurements were carried out for LDB1 KO and OE LDB1 HepG2 cells. (**B**) DEGs from RNA-seq for LDB1 KO and control HepG2 cells. Upregulated (red) and downregulated (blue) genes are shown. Examples of the top DEGs are labeled. (**C**) Heatmap of representative strongly up- or downregulated DEGs. Black triangles indicate genes looped to LDB1-binding enhancers in HepG2 cells. (**D**) Gene ontology (GO) analysis for DEGs in LDB1 KO HepG2 cells. Upregulated enriched pathways (red), downregulated enriched pathways (yellow) and significance of enrichment are shown. (**E**) Genomic features (%) of LDB1 peaks in HepG2 cells (FDR < 0.05). (**F**) Differentially enriched H3K27ac peaks between LDB1 KO and control HepG2 cells. Number of differential peaks and peaks with >2-fold change are shown. (**G**) Distribution of differential H3K27ac sites in genome. (**H**) Binary heatmap representing number of DEGs resulting from LDB1 loss that are looped to an enhancer or an LDB1-occupied enhancer.

LDB1 is recruited primarily to enhancers to regulate gene expression in HepG2 cells

To determine direct targets of LDB1 in HepG2 cells, LDB1 ChIP-seq was performed. The result revealed 3366 peaks (FDR < 0.05), of which very few (11.48%) were at promoters and ∼82% were in intergenic or intronic regions where enhancers are found (Figure 1E). In support, there was a 88% overlap of LDB1 peaks with enhancers called by EnhancerAtlas2.0 (19), similar to erythroid cells (Supplementary Figure S2A) (20).

To explore whether loss of LDB1 affected H3K27ac modification that marks both transcribed gene promoters and active enhancers, H3K27ac ChIP-seq was carried out for control and LDB1 KO HepG2 cells. We found differential H3K27ac binding at a relatively small number of sites (2348 diffbinds at FDR < 0.05) (Figure 1F). Moreover, only 348 H3K27ac peaks changed enrichment by at least 2-fold, with 70% of those changed peaks representing decreases in acetylation. Differential H3K27ac sites were common at both promoters (47%) and at intronic or intergenic locations (40%) (Figure 1G). Overlap of H3K27ac diffbinds with promoters (UCSC annotated promoters, −1 kb of TSS) was 40% (Supplementary Figure S2B). We found 116 DEGs associated with the lack of LDB1 that overlapped H3K27ac diffbinds ($\log_2$FC >0 or <0) (Supplementary Figure S2C). Up- or downregulated DEGs were highly correlated (R = 0.89) with increased or decreased H3K27ac, respectively. Overall, these results suggest that lack of LDB1 affects H3K27ac levels at enhancers and promoters, accompanied by changes in gene expression.

To identify the regulatory targets of enhancers that were occupied by LDB1, we intersected DEGs and genomic LDB1 localization with promoter-capture HiC data for adult human liver (21). This analysis revealed that among 490 DEGs upon LDB1 KO, 355 make long-range contact to a putative enhancer-containing fragment and 242 DEGs contact a putative enhancer fragment occupied by LDB1 (Figure 1H). LDB1 DEGs were enriched for loops to LDB1-occupied enhancers (P = 0.0199, odds ratio = 1.312, Fisher's exact test). Among the genes contacting these LDB1-binding enhancers are 18 out of the 32 genes strongly dysregulated by LDB1 KO in Figure 1C. There were 86 examples of DEGs linked to LDB1-bound enhancers that were H3K27ac diffbinds upon LDB1 loss. Examples include *ALCAM*, *SEMA6A* and *SLC2A2* enhancers (see below). Increased or decreased diffbind H3K27ac modification correlated (R = 0.52) with linked gene up- or downregulation (Supplementary Figure S2D). However, exceptions were notable, possibly due to linking of DEGs to more than one enhancer fragment (215 DEGs linked to 706 enhancers), which leaves indeterminant which contact(s) are functionally relevant. Overall, these results support the idea that LDB1 gene regulation in HepG2 cells is linked to long-range looping interactions and that loss of these interactions correlates with decreased H3H27ac and transcription at affected linked promoters.

Cooperation between LDB1 and master liver transcription factors to regulate liver genes

LDB1 depends on partner proteins to bind chromatin and regulate long-range gene transcription. *De novo* motif analysis of LDB1 binding sites in HepG2 cells using Homer (22) revealed that LDB1 peaks were enriched for the canonical GATA motif as well as motifs for the liver factors FOXA, TCF7 and HNF4 (Figure 2A). GATA4 and GATA6 DNA-binding proteins are required for development of the embryonic liver (23). However, in HepG2 cells, GATA4 was the only GATA factor with substantial expression (Supplementary Figure S2E). Moreover, GATA4 occupies thousands of sites in adult liver, supporting a role for GATA4 in liver gene expression (24).

LDB1 binding sites in HepG2 cells significantly overlapped with GATA4 sites (67%) obtained from published ChIP-seq data, providing evidence for both shared and independent functions for these factors (Supplementary Figure S2F). Strikingly, LDB1 and GATA4 co-occupancy was highly correlated with liver transcription factors TCF7, HNF4A and FOXA1 in terms of both localization and signal intensity, suggesting that LDB1 functions together with key hepatocyte factors in HepG2 cells to regulate gene expression (Figure 2B, Supplementary Figure S2F). We found 965 sites co-occupied by LDB1, TCF7, HNF4A, FOXA1 and GATA4 (Supplementary Figure S2G). The heatmap in Figure 2C illustrates two populations of LDB1 sites that we refer to as LDB1-only or LDB1 + GATA4 sites. Of note, both LDB1-only and LDB1 + GATA4 sites are occupied by liver transcription factors TCF7, HNF4A and FOXA1, although the density of liver factors at LDB1-only sites is considerably lower (Figure 2C).

We next asked whether there was a direct interaction between LDB1 and any of the liver transcription factors we observed to co-occupy regulatory sites. LDB1 IP successfully pulled down HNF4A and GATA4 but provided no evidence for interaction with FOXA1 or TCF7 (Figure 2D). Typically, LDB1 complexes require a LIM homeodomain partner to allow direct binding with DNA or a LIM-only protein to link it to additional partners to bind DNA. Based on the abundance of LMO7 RNA among LIM factors expressed in HepG2 cells (Supplementary Figure S2H), we carried out western blotting for this single LIM domain factor. The results revealed a strong interaction between LMO7 and LDB1 (Figure 2D).

ALCAM and *SEMA6A* are examples of DEGs with decreased expression upon LDB1 KO (Figure 1C). In particular, *ALCAM* and *SEMA6A* putative enhancers called by ChromHMM in HepG2 cells and displaying DNase I hypersensitivity and P300 occupancy are co-occupied by LDB1 and liver factors FOXA1, GATA4, HNF4A and TCF7 (Figure 2E and F). H3K27ac at the promoter and enhancers of these two genes is greatly reduced after LDB1 loss. Together, these experiments reveal a novel potential cooperation between LDB1 or LDB1 + GATA4 complexes and liver transcription factors to regulate a cohort of liver genes through their enhancers.

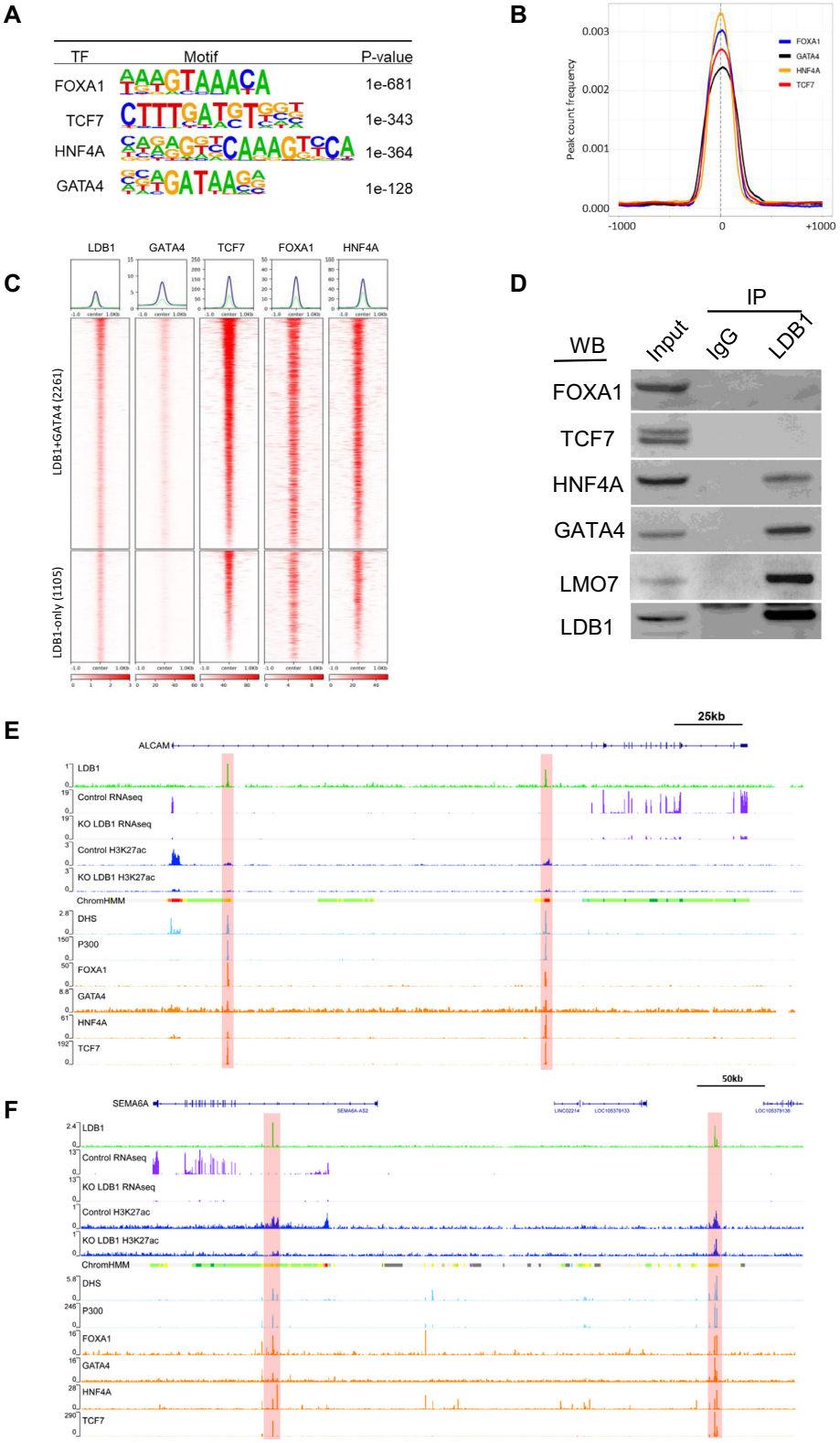

Figure 2. LDB1 cooperates with liver transcription factors to regulate gene expression. (**A**) Sequences and significance of enrichment of DNA motifs at LDB1 binding sites in HepG2 cells. (**B**) Distribution of liver transcription factors FOXA1, HNF4A, GATA4 and TCF7 peaks in a ±1 kb window of LDB1 binding sites. (**C**) Heatmaps showing distribution of liver transcription factors binding at LDB1 + GATA4 peaks and LDB1-only peaks. (**D**) IP of LDB1 in HepG2 cells. FOXA1, TCF7, HNF4A, GATA4, LMO7 and LDB1 were detected in LDB1 antibody pulldown by western blot. IgG served as control. RNA-seq for LDB1 KO and control cells and LDB1 and H3K27ac ChIP-seq peaks are visualized at the *ALCAM* (**E**) and *SEMA6A* gene loci (**F**). Enhancer marks (DHS and P300) and liver transcription factor peaks (FOXA1, GATA4, HNF4A and TCF7) are for HepG2 cells from ENCODE.

LDB1 regulates SLC2A2 expression by mediating enhancer–promoter interaction

The data so far strongly suggest that LDB1 regulates genes in HepG2 cells by mediating interactions between the genes and their enhancers. To further pursue this line of investigation, we focused on *SLC2A2*, which encodes GLUT2, the major glucose transporter in hepatocytes. In all four LDB1 KO clones, GLUT2 expression was strongly reduced with no effect on GLUT1 or GLUT3 expression (Figure 3A, Supplementary Figure S3A). Incubation of normal primary mouse hepatocytes or HepG2 cells in media containing a high concentration of glucose increases transcription of GLUT2 (Figure 3B) (25). However, this effect was abrogated in HepG2 cells lacking LDB1.

Publicly available ChIP-seq data and ChromHMM for HepG2 cells suggest localization of putative enhancers in the *SLC2A2* locus corresponding to H3K27ac, DNase I hypersensitivity and P300 binding (Figure 3C). We designated these positions E1–E4. Interestingly, the *SLC2A2* locus is flanked by insulator CTCF binding sites (CBS, Figure 3C) and an additional CBS lies between the promoter and putative enhancer E2. ChIP-qPCR validated that each of the putative enhancers, as well as the *SLC2A2* promoter, is occupied by LDB1 and GATA4 in control HepG2 cells, with significant reduction of the signals in LDB1 KO cells (Figure 3D and E). ChIP-qPCR also validated the presence of HNF4, FOXA1 and LMO7 at *SLC2A2* locus regulatory sites (Supplementary Figure S3B–D).

HNF4A was strongly reduced at E3 and the *SLC2A2* promoter after LDB1 KO and LMO7 was reduced at E1. FOXA1 occupancy was reduced at E2 after LDB1 KO but remained relatively high. Lack of LDB1 did not affect transcription of any of these liver factors (Supplementary Figure S3E). HAT P300, which catalyzes the H3K27ac mark, was detected at all the sites and was reduced after LDB1 KO (Supplementary Figure S3F). However, E3 was the only putative enhancer site that was strongly enriched for the H3K27ac activator mark, which was modestly reduced after LDB1 loss (Figure 3F). We then knocked out E3 by CRISPR/Cas9 editing in HepG2 cells and obtained two KO clones (Supplementary Figure S3G). RT-qPCR results indicated that GLUT2 gene expression was significantly decreased in E3 KO clones, supporting E3 enhancer activity (Figure 3G).

Using 3C, we examined whether the *SLC2A2* promoter interacts with E1, E2 and E3/4. We found that interactions with E1 and E3/4 were significantly reduced after LDB1 loss (Figure 3H). The locus flanking CTCF sites also contact the *SLC2A2* promoter, but these interactions were not affected by LDB1 loss. Interestingly, we observed an increased interaction of the *SLC2A2* promoter with the proximal CTCF site that lies between the promoter and E2 after loss of LDB1. Overall, these results suggest that LDB1 mediates long-range enhancer interactions between the *SLC2A2* promoter and enhancers E1–E4. Upon LDB1 loss, the promoter makes reduced contacts with E1 and E3/4 but increased contacts with a proximal CTCF site, which may interfere with E3/4 interactions and negatively affect gene expression (26). These results provide evidence that lack of LDB1 affects LDB1/GATA4 complex occupancy in the *SLC2A2* locus and that LDB1 functions as an enhancer looping protein in hepatocytes to regulate liver-expressed genes.

Conditional deletion of *Ldb1* in adult mouse liver improves metabolic parameters under HFD challenge

Hepatoma cell lines such as HepG2 and Hepa1-6 do not always accurately model hepatocyte function *in vivo* such as insulin sensitivity (27) and many protein-coding genes in liver are subject to species-specific regulation and function (28,29). However, the dysregulated metabolic gene expression and enhancer landscape upon LDB1 KO in HepG2 cells and colocalization between LDB1 and liver core transcription factors prompted us to explore whether LDB1 regulates metabolism *in vivo*. We first confirmed LDB1 expression in adult mouse hepatocytes by RNAscope. We found that LDB1 is expressed in hepatocytes in which Hnf4a is specifically expressed (Supplementary Figure S4A). Analysis of published mouse and human liver single-cell RNA-seq data (30,31) also indicated that LDB1 is expressed in mouse and human hepatocytes (Supplementary Figure S4B and C). LDB1 was selectively deleted in mouse hepatocytes by crossing $Ldb1^{fl/fl}$ mice with Albumin-Cre (*Alb*-cre) mice (Supplementary Figure S5A). The offspring were crossed with $Ldb1^{fl/fl}$ mice to obtain homozygous *Ldb1* conditional KO mice (hep-$Ldb1^{cKO}$) and $Ldb1^{fl/fl}$ control mice (Supplementary Figure S5B). When mice were 6 weeks old, *Ldb1* mRNA and protein levels were markedly reduced (Supplementary Figure S5C and D), as expected for excision by *Alb*-Cre (32).

To assess the role of LDB1 in hepatic glucose production, we isolated primary hepatocytes from hep-$Ldb1^{cKO}$ and $Ldb1^{fl/fl}$ control mice and measured glucose output *in vitro* (Supplementary Figure S5E). Upon stimulation with glucagon in the presence of gluconeogenic substrates, hep-$Ldb1^{cKO}$ and control hepatocytes secreted similar amounts of glucose, and insulin had no effect on this response. However, unstimulated hepatocytes from hep-$Ldb1^{cKO}$ animals produced more glucose than did $Ldb1^{fl/fl}$ control mice, suggesting that LDB1 may play a role in suppressing hepatic glucose production.

To investigate how loss of hepatic LDB1 protein might affect phenotypes under both normal and pathological conditions, hep-$Ldb1^{cKO}$ and $Ldb1^{fl/fl}$ control mice were maintained either on RC or HFD, which typically induces obesity and impaired glucose homeostasis. Since KO of Ldb1 in mouse liver enhances diethylnitrosamine-induced liver cancer, which may in turn affect liver metabolism, we checked for evidence of liver cancer in our RC and HFD Ldb1 KO mice by detecting cell proliferation and fibrosis. The results showed that there was no increase in cell proliferation or fibrosis in Ldb1 KO mouse liver under either RC or HFD feeding (Supplementary Figure S6A and B). RC hep-$Ldb1^{cKO}$ and $Ldb1^{fl/fl}$ control mice had equivalent body weight and fat mass (Supplementary Figure S7A). Similarly, blood glucose and serum insulin, TG, cholesterol and FFA levels were unchanged in hep-$Ldb1^{cKO}$ animals compared to control mice (Supplementary Figure S7B). In contrast, under HFD conditions, hep-$Ldb1^{cKO}$ mice showed reduced body weight and fat mass (Supplementary Figure S7C). The difference in body weight became significant af-

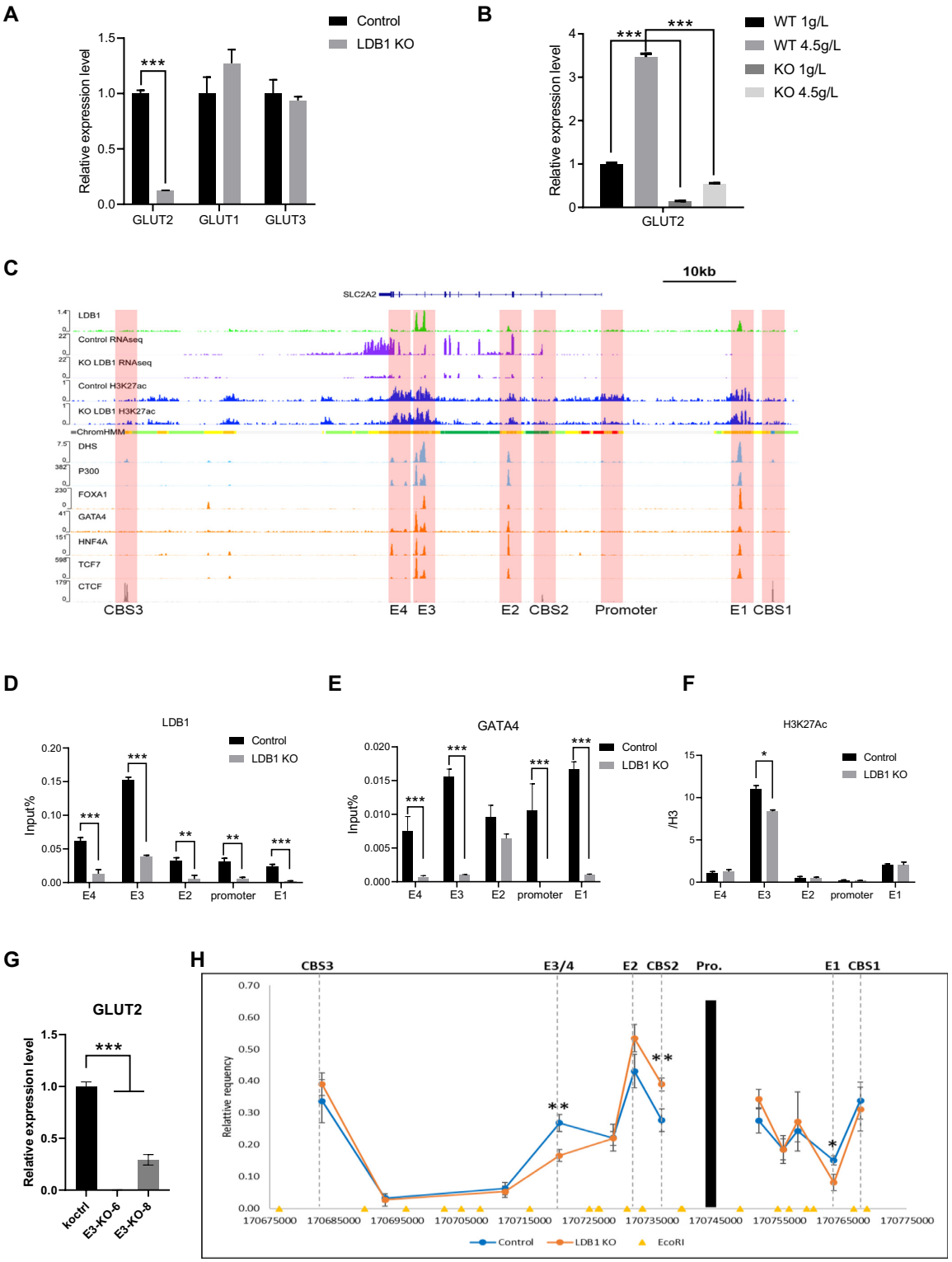

Figure 3. LDB1 regulates *SLC2A2* gene expression by mediating enhancer–promoter interaction. (**A**) RT-qPCR showing expression of GLUT1, GLUT2 or GLUT3 in LDB1 KO HepG2 cells. (**B**) RT-qPCR of GLUT2 expression after culture of control or LDB1 KO HepG2 cells under high (4.5 g/l) or low (1 g/l) glucose conditions. (**C**) Landscape of *SLC2A2* gene locus in HepG2 cells. LDB1, H3K27ac ChIP-seq and RNA-seq signals are shown. Enhancer marks (DHS and P300), liver transcription factors (FOXA1, GATA4, HNF4A and TCF7) and CTCF binding data are from ENCODE. The enhancer elements (E1–E4), CTCF binding sites (CBS1–3) and *SLC2A2* promoter are highlighted. ChIP-qPCR for LDB1 (**D**), GATA4 (**E**) and H3K27ac (**F**) in the *SLC2A2* locus in control and LDB1 KO HepG2 cells. (**G**) GLUT2 gene expression was detected in GLUT2 E3 KO HepG2 clones. (**H**) 3C in control and LDB1 KO HepG2 cells. EcoRI was used to digest chromatin. Anchor fragment (Pro.) contained the *SLC2A2* gene promoter, and interaction frequencies between the promoter and enhancers (E1–E4) or CTCF binding sites (CBS1–3) were detected by qPCR. Yellow triangles indicate EcoRI sites. The coordinates of the gene locus are shown on bottom of the graph. $N = 3$ for ChIP and 3C experiments.

ter 8 weeks of HFD feeding, while no significant weight difference was observed for RC feeding (Supplementary Figure S7D). Moreover, HFD hep-*Ldb1*^{cKO} mice displayed reduced serum TG levels (Supplementary Figure S7E).

We next analyzed glucose metabolism in hep-*Ldb1*^{cKO} and *Ldb1*$^{fl/fl}$ control mice under different diet conditions. RC hep-*Ldb1*^{cKO} animals developed glucose intolerance (IGTT), indicating that hepatocyte *Ldb1* expression is required for normal glucose homeostasis (Figure 4A). Hep-*Ldb1*^{cKO} mice also had significantly elevated blood glucose levels after administration of pyruvate, a substrate of gluconeogenesis (PTT), further supporting a role for LDB1 in hepatic glucose production. Plasma insulin levels were slightly elevated during the IGTT in RC hep-*Ldb1*^{cKO} mice (Figure 4A). However, ITT did not detect any differences in insulin sensitivity between the two and glucagon-induced increases in glucose levels (GCT) were similar in hep-*Ldb1*^{cKO} and *Ldb1*$^{fl/fl}$ mice genotypes (Supplementary Figure S8A and B). In contrast, HFD hep-*Ldb1*^{cKO} mice exhibited strikingly different phenotypes, compared to RC mutant mice. Hep-*Ldb1*^{cKO} animals on HFD showed improved glucose tolerance (IGTT) and increased insulin sensitivity (ITT), compared to HFD *Ldb1*$^{fl/fl}$ control mice (Figure 4B). HFD hep-*Ldb1*^{cKO} mice showed lower blood glucose levels after glucagon stimulation (Supplementary Figure S8C), while glucose excursions were similar in response to pyruvate (PTT) treatment (Supplementary Figure S8D). Together, these results indicate complex, diet-dependent effects of LDB1 loss on mouse liver metabolic functions.

Liver TG and cholesterol levels were similar in RC hep-*Ldb1*^{cKO} and control mice (Figure 4C). As expected, HFD feeding increased hepatic TG content in both genotypes (Figure 4D). However, hepatic TG levels (and plasma TG levels, Supplementary Figure S7E) were significantly lower in HFD hep-*Ldb1*^{cKO} mice, compared to HFD *Ldb1*$^{fl/fl}$ controls (Figure 4D). Hepatic cholesterol levels did not differ between genotypes (Figure 4D). RC hep-*Ldb1*^{cKO} animals showed an increase in liver weight, compared to control mice (Figure 4C). However, HFD hep-*Ldb1*^{cKO} animals showed a reduction in liver weight (Figure 4D). Of note, the relatively small sample size of experimental animals used in our study may have failed to reveal some significant differences between hep-*Ldb1*^{cKO} and *Ldb1*$^{fl/fl}$ control mice. For example, there was a decrease of average TG levels in hep-*Ldb1*^{cKO} mouse liver under both HFD and RC feeding, but the difference only reached significance in HFD mice. A larger sample size may increase the power to detect an increased number of significant differences. Finally, we used H&E and ORO staining of liver sections to examine changes in liver cellularity and fat accumulation. The histological appearance of livers of animals on RC appeared similar in control and mutant mice (Figure 4E, Supplementary Figure S9). However, there was a striking reduction of fat droplet accumulation in livers of HFD hep-*Ldb1*^{cKO} mice (Figure 4E, Supplementary Figure S9). Overall, decreased fat deposition in the livers of HFD hep-*Ldb1*^{cKO}, compared to control mice, corresponded to improved glucose tolerance and insulin sensitivity, smaller liver size and reduced serum TG. These data indicate that lack of LDB1 significantly improves hepatic metabolic function under HFD.

Dysregulated metabolic gene expression in adult hep-*Ldb1*^{cKO} mice

To explore the cellular/molecular basis for the altered hepatocyte function observed in LDB1-depleted livers from HFD mice, we carried out RNA-seq using liver cells harvested from both RC and HFD hep-*Ldb1*^{cKO} and *Ldb1*$^{fl/fl}$ control mice. The expression of thousands of hepatic genes is typically altered after HFD feeding (33). This was also the case for hep-*Ldb1*^{cKO} and *Ldb1*$^{fl/fl}$ control mice ($P_{adj} < 0.1$) (Supplementary Figure S10A and B). GO analysis revealed similar enrichment of processes for the *Ldb1*$^{fl/fl}$ and hep-*Ldb1*^{cKO} livers (Supplementary Figure S10C). Most DEGs observed on HFD compared to RC were shared between hep-*Ldb1*^{cKO} and *Ldb1*$^{fl/fl}$ control liver cells (65–67%), but the remainder were uniquely dysregulated in either hep-*Ldb1*^{cKO} or *Ldb1*$^{fl/fl}$ control liver cells under HFD conditions compared to RC feeding (Supplementary Figure S10D). Most gene expression changes upon LDB1 loss were modest (<2-fold).

We intersected both sets of DEGs with promoter-capture HiC performed for hepatocytes from mice fed a lipid-rich diet comparable to an HFD used here or a carbohydrate-rich diet comparable to RC used here (33). We selected enhancers from these interacting fragments by filtering for H3K27ac and H3K4me1 enrichment. Motif analysis using Homer for the enhancers interacting with DEGs in common (3912) or unique to *Ldb1*$^{fl/fl}$ (2106) or hep-*Ldb1*^{cKO} (1890) hepatocytes revealed enrichment for liver factors (Supplementary Figure S10E), similar to HepG2 cells, and GATA factors, presumably reflecting occupancy by GATA4. In addition, the motif for NR5A2 was highly enriched. *NR5A2* encodes LRH-1, a liver cell receptor with a role in hepatic lipid storage (34). These data indicate that enhancers looped to LDB1 DEGs to regulate metabolic genes *in vivo* are enriched for liver transcription factors. The suggestion is that LDB1 is involved to mediate these long-range interactions, but this remains to be proven since LDB1 ChIP-seq in hepatocytes was unsuccessful.

We next compared the effect of genotype on hepatic gene expression in animals maintained on RC or HFD. There were 509 DEGs comparing hep-*Ldb1*^{cKO} and *Ldb1*$^{fl/fl}$ control animals maintained on RC ($P_{adj} < 0.1$) (Figure 5A). The magnitude of change in gene expression was relatively small (<2-fold). GO analysis showed that downregulated genes were associated with lipoprotein (e.g. *Lsr*, *Saa4*, *Selenos*) and lipid storage (e.g. *Mup1*) pathways (Figure 5B). Interestingly, upregulated genes were enriched for fatty acid metabolic processes (e.g. *Abhd1*, *Cyp2a22*, *Fads6*, *Acox1*). Intersection of these data with the promoter-capture HiC data revealed that putative enhancers interacting with these DEGs were enriched for liver transcription factors and NR5A2 (Figure 5C). The GATA3 motif was enriched ($P = 1e{-}2$), but the GATA4 motif was not. Considering the similarities of these motifs and the presence of GATA4 but not GATA3 in liver cells, we suggest that these motifs may be occupied by GATA4.

We found few DEGs under HFD conditions in livers of hep-*Ldb1*^{cKO} compared to control mice: 30 genes were upregulated and 24 genes were downregulated ($P_{adj} < 0.1$), again with relatively low fold change in gene expression

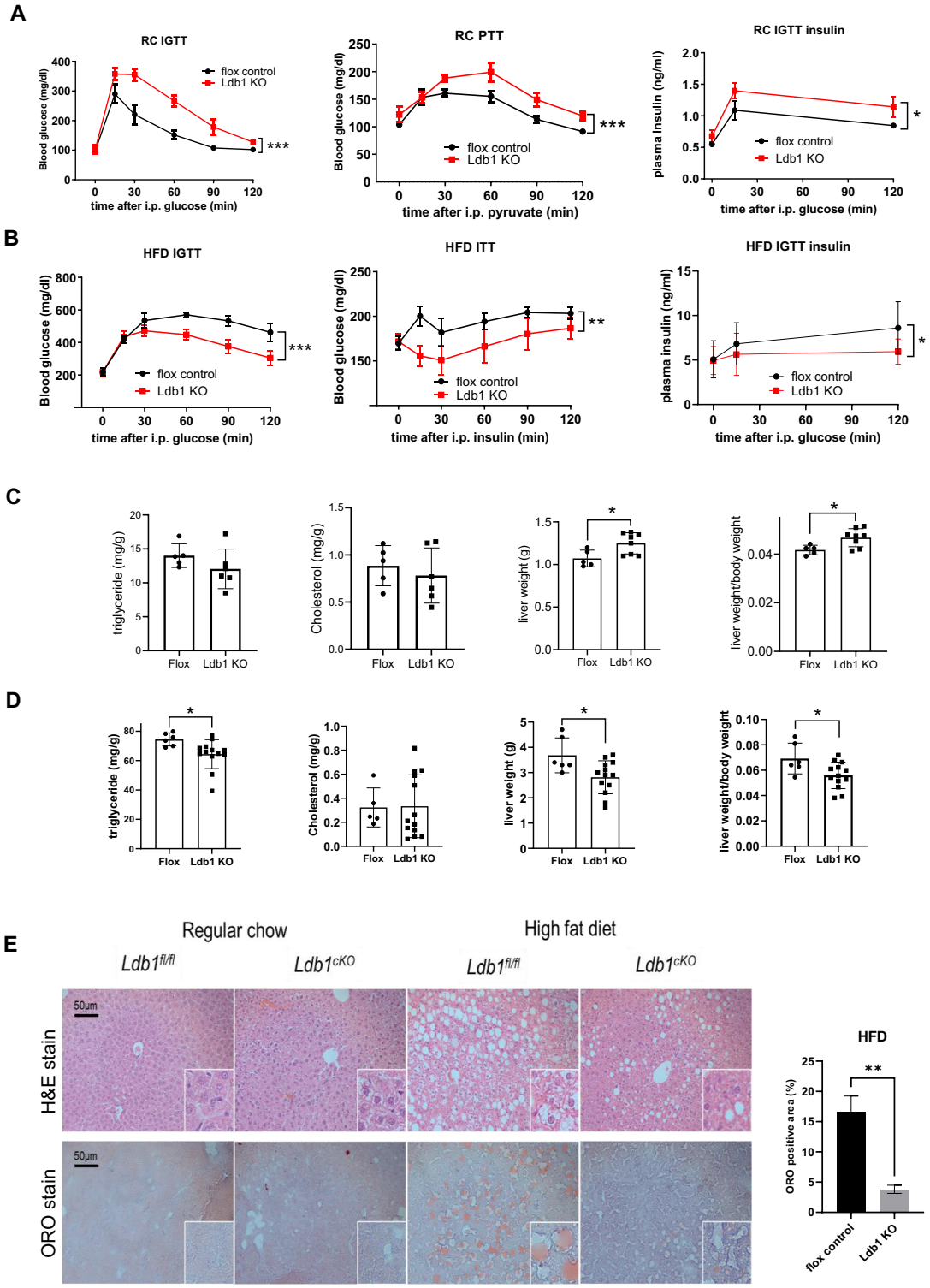

Figure 4. Metabolic analysis of hep-*Ldb1*^{cKO} mice. (**A**) IGTT, PTT and glucose-induced insulin secretion test were performed in control *Ldb1*$^{fl/fl}$ mice and hep-*Ldb1*^{cKO} mice fed RC. (**B**) IGTT, ITT and glucose-induced insulin secretion test were performed with control *Ldb1*$^{fl/fl}$ mice and hep-*Ldb1*^{cKO} mice maintained on HFD. All studies were carried out with hep-*Ldb1*^{cKO} male mice and *LDB1*$^{fl/fl}$ male littermates. For HFD studies, mice were fed RC for 8 weeks and then switched to the HFD for at least 11 weeks. Metabolic tests were performed with mice that were 19–22 weeks old ($N = 4$–7 per group). RC mice were subjected to metabolic tests when they were 7–12 weeks old ($N = 4$–7 per group). (**C**) Liver tissue analysis of control *Ldb1*$^{fl/fl}$ mice and hep-*Ldb1*^{cKO} mice fed with RC. (**D**) Liver tissue analysis of control *Ldb1*$^{fl/fl}$ mice and hep-*Ldb1*^{cKO} mice consuming HFD. Mice were maintained on the HFD for 16 weeks prior to collection of liver samples ($N = 5$–13 per group). Livers were isolated from RC mice at 12 weeks of age ($N = 5$–8 per group). (**E**) Hematoxylin and eosin (H&E) staining and Oil Red O (ORO) staining of liver sections collected from RC *Ldb1*$^{fl/fl}$ control and hep-*Ldb1*^{cKO} mice (12 weeks of age, $N = 5$) or after 15 weeks of HFD feeding (23 weeks of age, $N = 5$). The ratio of ORO staining area to parenchymal cell area was quantified with ImageJ.

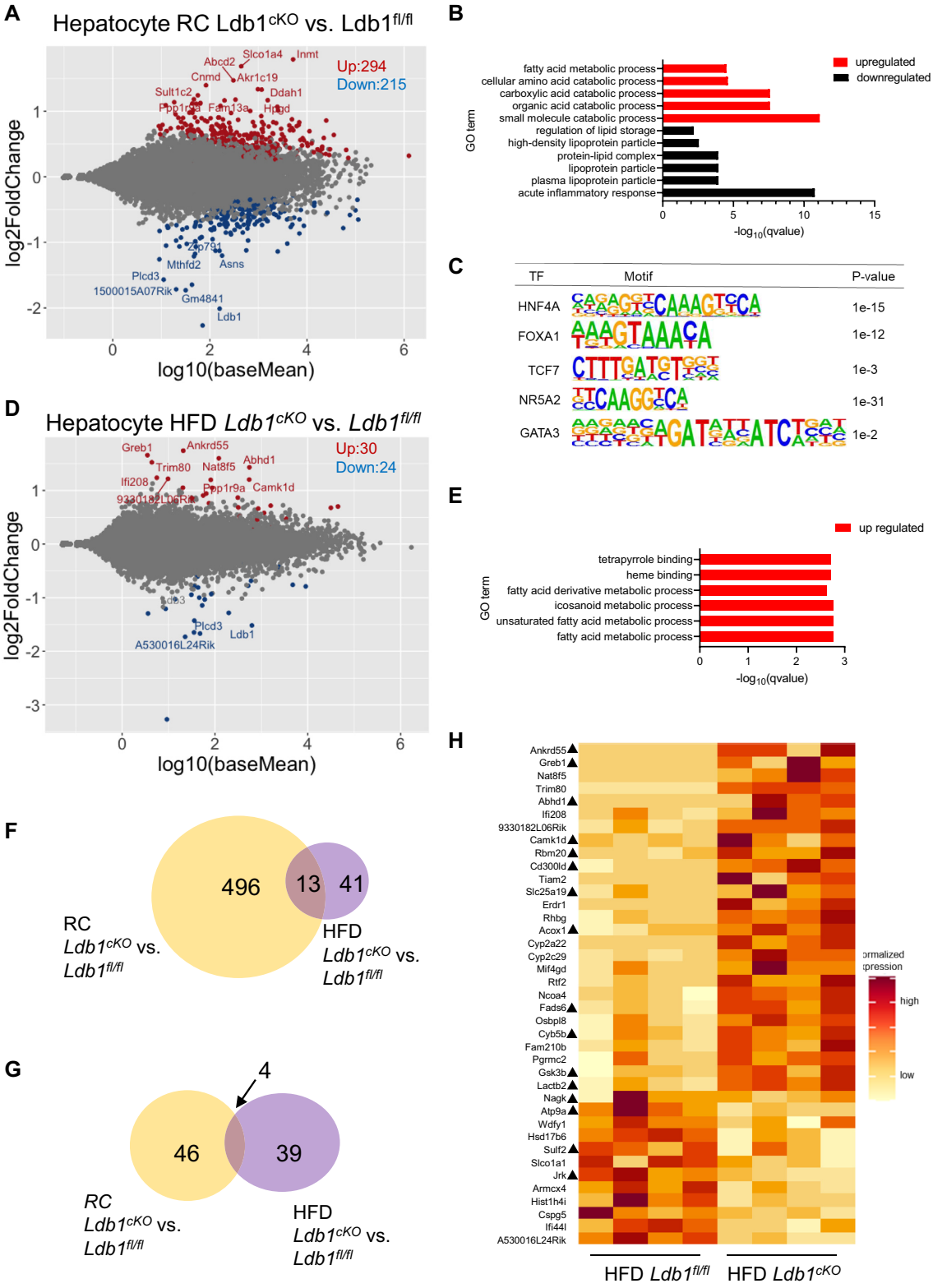

Figure 5. Altered gene expression in hep-*Ldb1*^{cKO} mouse hepatocytes. (**A**) DEGs of mouse livers collected from hep-*Ldb1*^{cKO} mice and *Ldb1*$^{fl/fl}$ control mice fed with RC. Upregulated (red) and downregulated (blue) genes are shown. Examples of top changed genes are labeled. (**B**) GO analysis for enriched pathways for DEGs in panel (A). Upregulated enriched pathways (red), downregulated enriched pathways (black) and significance of enrichment are shown. (**C**) Motif enriched in looped enhancer of DEGs in panel (A). (**D**) DEGs of mouse livers collected from hep-*Ldb1*^{cKO} mice and *Ldb1*$^{fl/fl}$ control mice fed with HFD. (**E**) GO analysis and significance of enrichment for DEGs from panel (C). Only upregulated genes showed enriched pathways. (**F**) Overlap of DEGs in panels (A) and (C). (**G**) Overlap of top 50 DEGs in panels (A) and (C). (**H**) Heatmap of unique DEGs under HFD conditions compared to RC feeding from panel (G). Black triangles indicate genes whose human orthologs have LDB1 binding at putative enhancer regions in HepG2 cells.

(Figure 5D). Upregulated genes were enriched for fatty acid metabolic process-related genes, similar to hep-*Ldb1*^{cKO} animals on RC (e.g. *Abhd1*, *Cyp2a22*, *Fads6*, *Acox1*) (Figure 5E). Downregulated genes did not display any enriched process groups, and lipoprotein process genes *Lsr*, *Saa4* and *Selenos* were not downregulated as they were in RC hep-*Ldb1*^{cKO} mice. About 24% of the DEGs comparing HFD hep-*Ldb1*^{cKO} and *Ldb1*$^{fl/fl}$ control mice were shared with RC DEGs (Figure 5F). Positive or negative effects of hepatocyte LDB1 loss on DEGs were highly correlated between the two diet conditions (Supplementary Figure S11A).

Consideration of the more highly affected DEGs upon LDB1 loss under RC or HFD conditions ($P_{adj} < 0.1$, top 50 DEGs with a symbol) revealed almost no overlap (Figure 5G). More of these DEGs were upregulated than were downregulated after LDB1 loss (Supplementary Figure S11B). To better understand the striking metabolic phenotypes of HFD hep-*Ldb1*^{cKO} mice, we focused on the 39 genes that were uniquely dysregulated on that diet condition in hep-*Ldb1*^{cKO} mice (Figure 5G). Among those, 28 named genes were upregulated and 11 were downregulated in the livers of HFD hep-*Ldb1*^{cKO} mice, as compared with *Ldb1*$^{fl/fl}$ mice (Figure 5H). We evaluated whether human orthologs of these genes showed peaks of occupancy by LDB1 in HepG2 cells. Forty-one percent of these genes showed one or more such peaks but LDB1 was seemingly not directly associated with the rest of the genes, although LDB1 may occupy their enhancers (Figure 5H). From these data, we conclude that the beneficial metabolic effects displayed by HFD hep-*Ldb1*^{cKO} mice may reflect both negative and positive regulation of gene expression by LDB1.

Conditional deletion of LDB1 in mouse hepatocytes changes the enhancer landscape

To explore how LDB1 conditional KO affects enhancer function in mouse hepatocytes, H3K27ac ChIP-seq was performed in RC hep-*Ldb1*^{cKO} and *Ldb1*$^{fl/fl}$ control mouse primary hepatocytes. We found 8175 H3K27ac differential binding sites (FDR < 0.05) (Figure 6A). Similar to HepG2 cell, most sites (91%) have decreased H3K27ac modification. Only a small portion of the sites display >2-fold change of H3K27ac modification (Figure 6A). Promoters were the most prominent location for H3K27ac diffbinds in hepatocytes, but among diffbinds with >2-fold change in H3K27ac, more were found at intergenic and intronic sites (51%) where enhancers are located (Figure 6B and C). We called 51 125 enhancers in hep-*Ldb1*^{cKO} by overlap of H3K4me1 and H3K27ac modifications from ENCODE. Of these, 11 272 (22%) were contained within 4769 (58%) of the diffbinds, indicating a large effect of LDB1 loss on the enhancer landscape. Motif analysis of the H3K27ac diffbinds using Homer revealed enrichment of motifs for liver transcription factors FOXA1, TCF7 and HNF4A (Figure 6D). Motifs containing the canonical GATA motif are presumably occupied by GATA4, as the only GATA factor expressed in liver cells. Published mouse liver ChIP-seq data for GATA4, FOXA1 and HNF4A indicated preferential colocalization with differentially occupied H3K27ac sites with decreased modification upon LDB1 loss (Figure 6E).

To understand how enhancers with differential H3K27ac modification affect target gene expression, genes looped to these enhancers were obtained by intersection with promoter-capture HiC data. The 11 272 differential H3K27ac enhancers were looped to 2415 genes. Comparison of these genes to LDB1 DEGs in hep-*Ldb1*^{cKO} liver cells revealed subsets of 29 downregulated genes and 37 upregulated genes that were looped to enhancers with decreased H3K27ac modification (Figure 6F). Among the upregulated genes are *Fasn* and *Acot4*, which are involved in fatty acyl-CoA biosynthesis and *Acox1* and *Adh5*, which are involved in fatty acid oxidation, consistent with the enriched process groups shown in Figure 5B. Putative enhancers of these genes lost H3K27ac even though transcription of the linked genes increased (Supplementary Figure S12). Altogether, LDB1 loss greatly affects the enhancer landscape in RC hep-*Ldb1*^{cKO}.

DISCUSSION

LDB1 is a protein that is critical for numerous developmental processes, including cardiogenesis, neurogenesis and hematopoiesis (9). Molecular studies revealed it to be a chromatin looping protein functioning to connect enhancers and genes through LIM-only and LIM homeodomain partners in various cell types (12,35–37). Here, we report the novel finding that LDB1 modulates hepatocyte gene expression by regulating enhancer–promoter looping. We demonstrated that LDB1 functions in concert with liver transcription factors GATA4, FOXA1, HNF4A and TCF7 to regulate hundreds of liver metabolic genes through their enhancers. Further, hep-*Ldb1*^{cKO} mice show glucose intolerance on RC, while demonstrating improved glucose tolerance on HFD, an effect that may be related to enhanced fatty acid metabolic pathway gene expression. Accordingly, hep-*Ldb1*^{cKO} mice maintained on HFD showed attenuated hepatic steatosis and related pathologies.

Cooperation between LDB1 and master liver transcription factors regulates liver gene expression

HNF4A preferentially occupies enhancers genome-wide in developing liver at E14.5 and in adult liver (38). Moreover, HNF4A and FOXA1 jointly occupy the liver enhancer repertoire as it transitions during development (39). We found that LDB1 primarily occupies enhancers together with liver-specific transcription factors FOXA1, HNF4A, TCF7 and GATA4 in HepG2 cells. LDB1 interacts with GATA4 and either directly or indirectly with HNF4A. Thus, one mode of LDB1 chromatin occupancy in hepatocytes may be through GATA4, analogous to GATA1 interaction in erythroid cells, which depends on the bridging function of LMO2 (12). Our RNA-seq data showed that the only LIM domain protein transcribed at substantial levels in HepG2 cells or in mouse hepatocytes *in vivo* is LMO7, which has only one LIM domain. We observed strong interactions of LMO7 with LDB1.

LMO7 is a target of TGF-β and is involved in the development of many cancers, including hepatomas, and is positively correlated with the invasive capacity of hepatoma cells (40). In muscle cells, LMO7 interacts with emerin, which

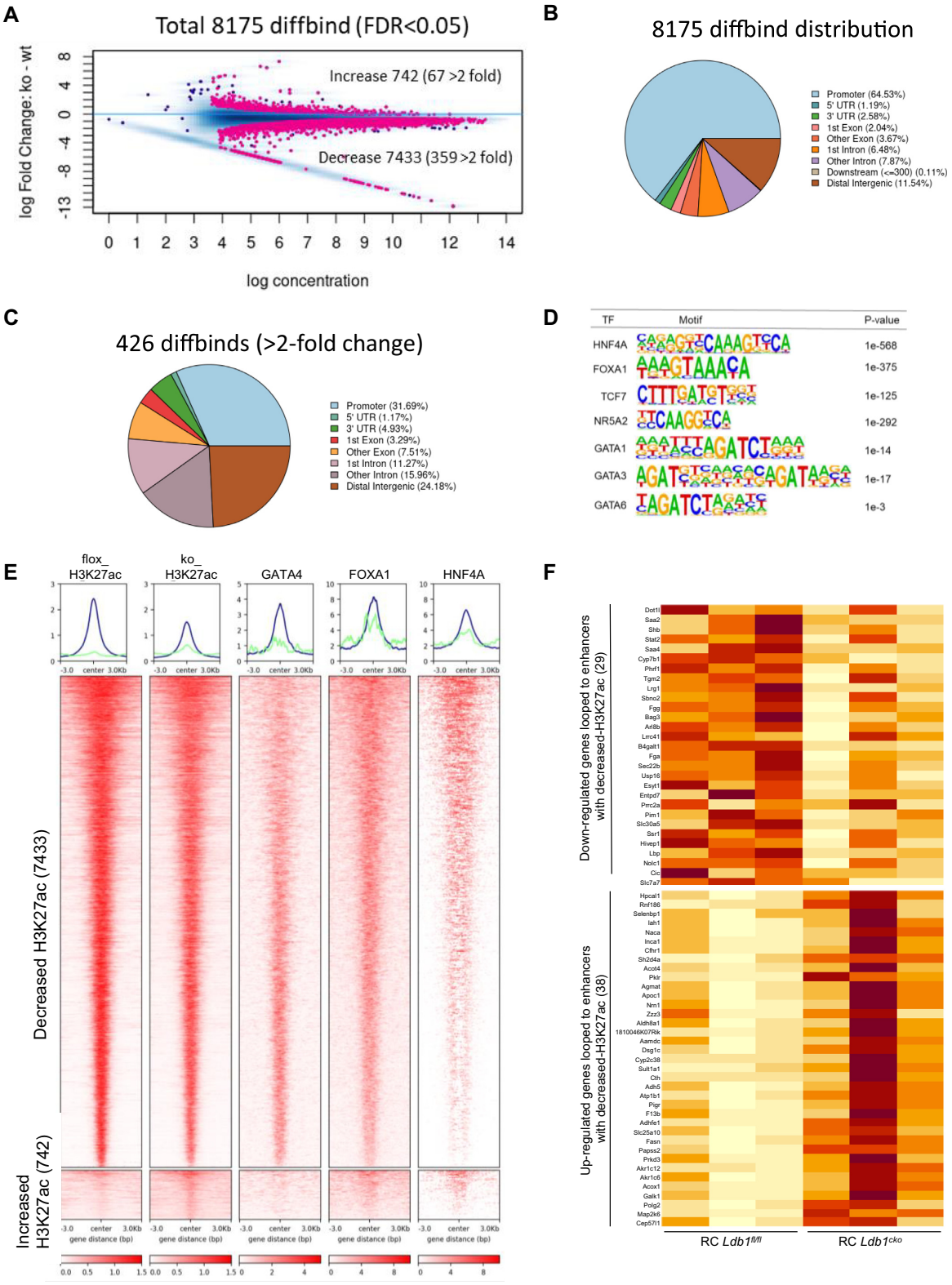

Figure 6. H3K27ac modification changes in hep-*Ldb1*^{cKO} mouse hepatocytes. (**A**) Differentially enriched H3K27ac peaks between *Ldb1*$^{fl/fl}$ control and hep-*Ldb1*^{cKO} mouse hepatocytes. Number of differential peaks and peaks with >2-fold change are shown. (**B**) Distribution of differential H3K27ac sites in genome. (**C**) Distribution of differential H3K27ac sites with >2-fold change in genome. (**D**) Motif enrichment of liver transcription factors in differential H3K27ac sites. (**E**) Heatmaps showing binding of liver transcription factors at decreased and increased H3K27ac sites. (**F**) Gene expression heatmap showing DEGs in RC hep-*Ldb1*^{cKO} mouse hepatocytes that looped to enhancers with decreased H3K27ac modification.

belongs to the LEM domain family and binds to the BAF complex to regulate chromatin structure (41). The mechanism by which LMO7 can affect cell proliferation is still unclear. Since KO of Ldb1 in mouse liver enhances cancer development (10), the interaction between LDB1 and LMO7 that we demonstrated in liver cells may contribute to this process. A second mode of LDB1 chromatin binding is through a LIM homeodomain protein, exemplified by LDB1–ISL1 interaction in diverse tissues (35,36,42). However, LIM homeodomain proteins were almost undetectable in HepG2 cells or in hepatocytes *in vivo*, making this mode of LDB1 function unlikely.

Our ChIP-seq data obtained with HepG2 cells revealed that LDB1 peaks were predominantly at enhancers and that half of the LDB1 peaks were co-occupied by GATA4. Both LDB1 + GATA4 peaks and LDB1-only peaks were enriched for liver transcription factors. To obtain LDB1 enhancers in hepatocytes, we intersected DEGs of hep-*Ldb1*^{cKO} with promoter-capture HiC data for hepatocytes from mice fed diets equivalent to those used in the present study (RC and HFD) (33). More than 900 presumptive LDB1-bound enhancers were obtained that were highly enriched for HNF4A, FOXA1, TCF7 and the canonical GATA motifs.

Interestingly, the NR5A2 motif was highly enriched at these enhancers. NR5A2 encodes LRH-1, a liver cell receptor whose target genes are involved in hepatic cholesterol uptake and efflux, HDL formation and cholesterol exchange between lipoproteins and fatty acid synthesis. LRH-1 controls the first step of hepatic glucose uptake through direct transcriptional regulation of the glucokinase gene (43). LRH-1 and HNF4A cooperate in regulating the Cyp7a1 gene that encodes the first and rate-limiting enzyme in the major bile acid synthetic pathway and promotes active transcription histone marks on the Cyp7a1 promoter (44). We found that Cyp7a1 gene expression in LDB1 KO mouse liver was increased under RC feeding and that the LRH-1 binding motif was enriched in LDB1 presumptive enhancers, suggesting that LDB1 cooperates with LRH-1 to regulate gene expression.

Nr5a2 KO mice on an HFD develop steatosis and become glucose intolerant (34), which are sequelae of HFD consumption that are greatly attenuated in HFD *Ldb1* KO mice. Indeed, a comparison of our *Ldb1* KO RNA-seq data with the corresponding *Nr5a2* KO data revealed co-regulation of 72 genes, most of which (61%) were upregulated by *Ldb1* KO and downregulated by *Nr5a2* KO, potentially explaining the opposite effect of their loss on HFD-induced hepatic steatosis. Examples include *Elovl5* and *Fads2*, well-known targets of NR5A2, that were oppositely regulated by LDB1 and NR5A2 KO under both diet conditions (RC and HFD).

LDB1-only peaks may represent a novel type of LDB1 enhancer binding complex whose interaction with chromatin remains to be further explored. HNF4A function may be important for LDB1 complexes in liver cells, since HNF4A recruitment to LDB1 sites in the *SLC2A2* locus was reduced after LDB1 KO. HNF4A binds DNA as a homodimer, and chromatin residence could be stabilized by LDB1. In contrast, the liver transcription factor FOXA1 remains bound in the *SLC2A2* locus in the absence of LDB1, consistent with binding of this pioneer transcription factor being an early event in LDB1 enhancer activation and with data showing the HNF4A binding is dependent on the presence of FOXA factors at co-bound sites in liver cells (45). Both FOXA factors and HNF4A contribute to maintaining enhancer activity in adult liver (45,46). Our findings provide evidence that LDB1 forms protein complexes with liver transcription factors to regulate metabolic gene expression in hepatocytes through co-occupancy at regulatory sites that are primarily enhancers.

Notably, KO of GATA4, or both GATA4 and GATA6 by intravenous injection of AAV8-Tbg-Cre, in adult mouse liver did not affect liver function although GATA4 ChIP-seq in hepatocytes revealed >4000 binding sites that were enriched for genes involved in lipid and glucose metabolism (24). Moreover, gene expression detected by microarray in GATA4 KO hepatocytes revealed 716 DEGs (FDR < 25%) that were enriched in liver function-associated pathways such as fatty acid beta oxidation and bile acid biosynthesis. However, DEGs upon GATA4 loss had little overlap with those found in hepatocytes from hep-*Ldb1*^{cKO} mice.

Compared to Alb-Cre, which we used in this study to excise Ldb1, AAV8-Tbg-Cre is more hepatocyte-specific (47). However, AAV8-Tbg-Cre can excise floxed sequences in cholangiocytes in neonatal mouse liver (48) and manipulation of mice with AAV8-Tbg-Cre can lead to reduction in liver proliferation together with induction of the DNA damage marker and transcriptional changes (47). These different Cre strategies may contribute to differences in hepatic gene expression. The lack of a liver phenotype in *Gata4* loss-of-function mice contrasts with the glucose intolerance we observed in RC hep-*Ldb1*^{cKO} mice, suggesting compensation *in vivo* for loss of the former but not the latter. Alternatively, a GATA4-independent function of LDB1 could underlie the phenotype we observed in RC hep-*Ldb1*^{cKO} mice. This possibility is supported by our observation that enhancers of LDB1 KO DEGs were not specifically enriched for the GATA4 motif. *Gata4* loss-of-function mice were not subjected to HFD feeding, which could reveal whether the pathology-sparing effect of *Ldb1* ablation upon HFD feeding is shared with *Gata4*.

LDB1 regulates metabolic genes, including *SLC2A2*, by mediating enhancer looping

We found numerous liver genes that were dysregulated by loss of LDB1 whose enhancers or putative enhancers were occupied by LDB1 together with liver transcription factors FOXA1, HNF4A, GATA4 and TCF7. To establish the mechanism underlying this regulation, we focused on GLUT2, encoded by *SLC2A2*. GLUT2 is expressed in various cell types, including hepatocytes and pancreatic β cells, and functions as a glucose sensor. Loss of GLUT2 leads to early-onset diabetes in mice (49). Using our ChIP-qPCR and published data from ENCODE for HepG2 cells, we observed that liver factors HNF4A, FOXA1, TCF7 and GATA4 co-occupy the *SLC2A2* promoter and putative enhancers with LDB1. The enhancers loop to the *SLC2A2* promoter and lack of LDB1 disrupted the loops and *SLC2A2* transcription.

Interestingly, when *Ldb1* was ablated in mouse liver, RC mice became glucose intolerant and showed increased glucose-stimulated insulin secretion, suggestive of insulin resistance. This phenotype was also observed after *Ldb1* ablation in pancreatic islet β cells in which RNA-seq indicated dysregulation of the transcription factor network that establishes and maintains islet β cell fate, including downregulation of *Slc2a2* (42). Ablation of *Isl1* in islet β cells in this study phenocopied the *Ldb1* loss of function on RC, providing strong evidence that LDB1 and ISL1 function together in these cells. Moreover, a putative *Slc2a2* enhancer, which is conserved in human cells (E1, in our study), is occupied by LDB1, ISL1 and islet factors PDX1, NKX2.2, NKX6.1 and FOXA2 in islet β cells. However, while *SLC2A2* was downregulated upon LDB1 loss in β cells and HepG2 cells, it was unchanged in hep-*Ldb1*^{cKO}, suggesting that LDB1 loss can be compensated *in vivo*, at least in the case of *Slc2a2*. Together, these data suggest regulation of *Slc2a2* expression in pancreatic β cells and hepatocytes by different tissue-specific LDB1 complexes. We demonstrated that the LDB1 complex regulates *SLC2A2* in HepG2 cells by mediating enhancer looping. A similar mechanism is likely to be operative in β cells, although the LDB1 LIM domain partner is different (42).

LDB1 regulates metabolism in adult mouse liver cells

Recent studies have indicated the importance of LDB1 in regulating the function of metabolic tissues and cell types. Endocrine cell-specific *Ldb1*^{cKO} mice showed decreased numbers of pancreatic islet α, β and γ cells (50). KO of *Ldb1* in adult mouse pancreatic β cells resulted in defective insulin secretion and glucose homeostasis (42). Global heterozygous *Ldb1*$^{+/-}$ mice maintained normal glucose homeostasis but had improved insulin sensitivity along with defects in energy expenditure and altered metabolic gene expression in brown adipose tissue (51). These authors also observed improved insulin sensitivity with no change in energy balance in inducible β-cell-specific *Ldb1* KO mice. However, it remained unclear whether LDB1 might affect metabolic functions of adult hepatocytes.

We found that RC hep-*Ldb1*^{cKO} mice became glucose intolerant. Moreover, hepatocytes from hep-*Ldb1*^{cKO} mice showed increased glucose output and gluconeogenesis, as compared to control hepatocytes. In agreement with this observation, treatment of hep-*Ldb1*^{cKO} mice with pyruvate resulted in significantly elevated blood glucose levels. Hundreds of genes that are enriched for metabolic pathways were dysregulated in RC hep-*Ldb1*^{cKO} mice. Among these, some catabolic processes were upregulated, while lipid storage-related processes were downregulated. This result supports the idea that changes in gene expression may underlie the metabolic phenotype of RC hep-*Ldb1*^{cKO} mice but also suggests that the phenotype is likely to be the outcome of complex changes in the expression of multiple genes, most probably also involving resulting compensatory responses.

LDB1 loss resulted in decreased H3K27ac at the GLUT2 enhancers, reduced looping to the promoter and reduced transcription in HepG2 cells. However, in hepatocytes, while almost all enhancers lost H3K27ac, there were only a limited number of Ldb1 DEGs that displayed increased or decreased expression. The results are consistent with recent reports showing that reduction of H3K27ac at enhancers may not always have major effects on gene transcription and can result in both up- and downregulation of genes (52,53). The molecular mechanisms involved in these processes remain unknown. In erythroid cells, predominance of co-repressor ETO2 over Ldb1 in the Ldb1 complex switches the activity of the complex from positive to negative regulation of target genes (54–57). Future studies involving the endogenous tagging of Ldb1 should facilitate localization of the protein in the genome to determine direct targets and identify repressive protein components in the LDB1 complex in liver cells.

Unexpectedly, relatively few genes were significantly dysregulated in HFD hep-*Ldb1*^{cKO} mice. Nevertheless, the obesity, liver steatosis and insulin resistance associated with HFD were greatly attenuated in HFD hep-*Ldb1*^{cKO} mice. The upregulated fatty acid metabolic process genes (Abhd1, Cyp2a22, Fads6, Acox1, Akr1c19, Cyp2c29) in HFD hep-*Ldb1*^{cKO} mice may contribute to the phenotype. *Acox1*, which is the first rate-limiting enzyme in the fatty acid beta-oxidation pathway, was among the top 50 upregulated genes in HFD hep-*Ldb1*^{cKO} mice but not in RC mice. Also, lipoprotein process genes *Lsr*, *Saa4* and *Selenos* were not downregulated as they were in RC hep-*Ldb1*^{cKO} mice. It appears that both up- and downregulated genes upon LDB1 loss may be relevant to the improved liver phenotype observed on HFD, supporting the idea that the phenotype is likely to be the result of complex changes in gene expression networks governing physiological changes. Further studies in the future will be needed to identify the molecular basis of the observed metabolic phenotypes of hep-*Ldb1*^{cKO} mice and to clarify how LDB1 loss ameliorates liver steatosis in mice caused by an obesogenic diet. It is possible that Ldb1 could emerge as a potential target to reduce the negative outcomes of obesity or fatty liver disease.

DATA AVAILABILITY

Genome browser views for LDB1 and H3K27ac ChIP-seq and liver transcription factors are available in UCSC Genome Browser trackhub: http://genome.ucsc.edu/s/Guoyou_Liu/LDB1_liver_mm10, http://genome.ucsc.edu/s/Guoyou_Liu/LDB1_liver_hg38. Accession number of GEO: GSE179845.

SUPPLEMENTARY DATA

Supplementary Data are available at NAR Online.

ACKNOWLEDGEMENTS

We thank Dr Lu Zhu for instructions in the collection of mouse hepatocytes. We thank Drs Cameron Palmer and Guoyun Yu for bioinformatics analysis, Dr Harold Brown and the NIDDK Genomics Core for sequencing, and Oksana Gavrilova and NIDDK Mouse Metabolism Core for *in vivo* phenotyping and biochemical assays on *Ldb1*$^{fl/fl}$ and hep-*Ldb1*$^{ko/ko}$ mice.

Author contributions: G.L. contributed to the conception, design, performance of experiments, analysis and interpretation of data, and writing the manuscript; L.W. contributed to the performance of experiments, and analysis and interpretation of data; J.W. contributed to critical review of the manuscript; and A.D. supervised the project and wrote the manuscript.

FUNDING

National Institute of Diabetes and Digestive and Kidney Diseases [DK 075033 to A.D.]. Funding for open access charge: National Institute of Diabetes and Digestive and Kidney Diseases.
Conflict of interest statement. None declared.

REFERENCES

1. Dixon,J.R., Selvaraj,S., Yue,F., Kim,A., Li,Y., Shen,Y., Hu,M., Liu,J.S. and Ren,B. (2012) Topological domains in mammalian genomes identified by analysis of chromatin interactions. *Nature*, **485**, 376–380.
2. Nora,E.P., Lajoie,B.R., Schulz,E.G., Giorgetti,L., Okamoto,I., Servant,N., Piolot,T., van Berkum,N.L., Meisig,J., Sedat,J. *et al.* (2012) Spatial partitioning of the regulatory landscape of the X-inactivation centre. *Nature*, **485**, 381–385.
3. Rao,S.S.P., Huang,S.C., St Hilaire,B.G., Engreitz,J.M., Perez,E.M., Kieffer-Kwon,K.R., Sanborn,A.L., Johnstone,S.E., Bascom,G.D., Bochkov,I.D. *et al.* (2017) Cohesin loss eliminates all loop domains. *Cell*, **171**, 305–320.
4. Plank,J.L. and Dean,A. (2014) Enhancer function: mechanistic and genome-wide insights come together. *Mol. Cell*, **55**, 5–14.
5. van Arensbergen,J., van Steensel,B. and Bussemaker,H.J. (2014) In search of the determinants of enhancer–promoter interaction specificity. *Trends Cell Biol.*, **24**, 695–702.
6. Javierre,B.M., Burren,O.S., Wilder,S.P., Kreuzhuber,R., Hill,S.M., Sewitz,S., Cairns,J., Wingett,S.W., Varnai,C., Thiecke,M.J. *et al.* (2016) Lineage-specific genome architecture links enhancers and non-coding disease variants to target gene promoters. *Cell*, **167**, 1369–1384.
7. Maurano,M.T., Humbert,R., Rynes,E., Thurman,R.E., Haugen,E., Wang,H., Reynolds,A.P., Sandstrom,R., Qu,H., Brody,J. *et al.* (2012) Systematic localization of common disease-associated variation in regulatory DNA. *Science*, **337**, 1190–1195.
8. Liu,G. and Dean,A. (2019) Enhancer long-range contacts: the multi-adaptor protein LDB1 is the tie that binds. *Biochim. Biophys. Acta Gene Regul. Mech.*, **1862**, 625–633.
9. Mukhopadhyay,M., Teufel,A., Yamashita,T., Agulnick,A.D., Chen,L., Downs,K.M., Schindler,A., Grinberg,A., Huang,S.P., Dorward,D. *et al.* (2003) Functional ablation of the mouse Ldb1 gene results in severe patterning defects during gastrulation. *Development*, **130**, 495–505.
10. Teufel,A., Maass,T., Strand,S., Kanzler,S., Galante,T., Becker,K., Strand,D., Biesterfeld,S., Westphal,H. and Galle,P.R. (2010) Liver-specific Ldb1 deletion results in enhanced liver cancer development. *J. Hepatol.*, **53**, 1078–1084.
11. Zhao,Y., Kwan,K.M., Mailloux,C.M., Lee,W.K., Grinberg,A., Wurst,W., Behringer,R.R. and Westphal,H. (2007) LIM-homeodomain proteins Lhx1 and Lhx5, and their cofactor Ldb1, control Purkinje cell differentiation in the developing cerebellum. *Proc. Natl Acad. Sci. U.S.A.*, **104**, 13182–13186.
12. Krivega,I., Dale,R.K. and Dean,A. (2014) Role of LDB1 in the transition from chromatin looping to transcription activation. *Genes Dev.*, **28**, 1278–1290.
13. Burant,C.F., Sreenan,S., Hirano,K., Tai,T.A., Lohmiller,J., Lukens,J., Davidson,N.O., Ross,S. and Graves,R.A. (1997) Troglitazone action is independent of adipose tissue. *J. Clin. Invest.*, **100**, 2900–2908.
14. Li,P., Ruan,X., Yang,L., Kiesewetter,K., Zhao,Y., Luo,H., Chen,Y., Gucek,M., Zhu,J. and Cao,H. (2015) A liver-enriched long non-coding RNA, lncLSTR, regulates systemic lipid metabolism in mice. *Cell Metab.*, **21**, 455–467.
15. Krivega,I. and Dean,A. (2018) Chromatin immunoprecipitation (ChIP) with erythroid samples. *Methods Mol. Biol.*, **1698**, 229–236.
16. Schmidl,C., Rendeiro,A.F., Sheffield,N.C. and Bock,C. (2015) ChIPmentation: fast, robust, low-input ChIP-seq for histones and transcription factors. *Nat. Methods*, **12**, 963–965.
17. Krivega,I. and Dean,A. (2018) Chromosome conformation capture (3C and higher) with erythroid samples. *Methods Mol. Biol.*, **1698**, 237–243.
18. Sefried,S., Haring,H.U., Weigert,C. and Eckstein,S.S. (2018) Suitability of hepatocyte cell lines HEPG2, AML12 and THLE-2 for investigation of insulin signalling and hepatokine gene expression. *Open Biol.*, **8**, 180147.
19. Gao,T. and Qian,J. (2020) EnhancerAtlas 2.0: an updated resource with enhancer annotation in 586 tissue/cell types across nine species. *Nucleic Acids Res.*, **48**, D58–D64.
20. Lee,J., Krivega,I., Dale,R.K. and Dean,A. (2017) The LDB1 complex co-opts CTCF for erythroid lineage-specific long-range enhancer interactions. *Cell Rep.*, **19**, 2490–2502.
21. Jung,I., Schmitt,A., Diao,Y., Lee,A.J., Liu,T., Yang,D., Tan,C., Eom,J., Chan,M., Chee,S. *et al.* (2019) A compendium of promoter-centered long-range chromatin interactions in the human genome. *Nat. Genet.*, **51**, 1442–1449.
22. Heinz,S., Benner,C., Spann,N., Bertolino,E., Lin,Y.C., Laslo,P., Cheng,J.X., Murre,C., Singh,H. and Glass,C.K. (2010) Simple combinations of lineage-determining transcription factors prime *cis*-regulatory elements required for macrophage and B cell identities. *Mol. Cell*, **38**, 576–589.
23. Watt,A.J., Zhao,R., Li,J. and Duncan,S.A. (2007) Development of the mammalian liver and ventral pancreas is dependent on GATA4. *BMC Dev. Biol.*, **7**, 37.
24. Zheng,R., Rebolledo-Jaramillo,B., Zong,Y., Wang,L., Russo,P., Hancock,W., Stanger,B.Z., Hardison,R.C. and Blobel,G.A. (2013) Function of GATA factors in the adult mouse liver. *PLoS One*, **8**, e83723.
25. Im,S.S., Kang,S.Y., Kim,S.Y., Kim,H.I., Kim,J.W., Kim,K.S. and Ahn,Y.H. (2005) Glucose-stimulated upregulation of GLUT2 gene is mediated by sterol response element-binding protein-1c in the hepatocytes. *Diabetes*, **54**, 1684–1691.
26. Huang,H., Zhu,Q., Jussila,A., Han,Y., Bintu,B., Kern,C., Conte,M., Zhang,Y., Bianco,S., Chiariello,A.M. *et al.* (2021) CTCF mediates dosage- and sequence-context-dependent transcriptional insulation by forming local chromatin domains. *Nat. Genet.*, **53**, 1064–1074.
27. Molinaro,A., Becattini,B. and Solinas,G. (2020) Insulin signaling and glucose metabolism in different hepatoma cell lines deviate from hepatocyte physiology toward a convergent aberrant phenotype. *Sci. Rep.*, **10**, 12031.
28. Jiang,C., Li,P., Ruan,X., Ma,Y., Kawai,K., Suemizu,H. and Cao,H. (2020) Comparative transcriptomics analyses in livers of mice, humans, and humanized mice define human-specific gene networks. *Cells*, **9**, 2566.
29. Yu,Y., Ping,J., Chen,H., Jiao,L., Zheng,S., Han,Z.G., Hao,P. and Huang,J. (2010) A comparative analysis of liver transcriptome suggests divergent liver function among human, mouse and rat. *Genomics*, **96**, 281–289.
30. MacParland,S.A., Liu,J.C., Ma,X.Z., Innes,B.T., Bartczak,A.M., Gage,B.K., Manuel,J., Khuu,N., Echeverri,J., Linares,I. *et al.* (2018) Single cell RNA sequencing of human liver reveals distinct intrahepatic macrophage populations. *Nat. Commun.*, **9**, 4383.
31. Su,Q., Kim,S.Y., Adewale,F., Zhou,Y., Aldler,C., Ni,M., Wei,Y., Burczynski,M.E., Atwal,G.S., Sleeman,M.W. *et al.* (2021) Single-cell RNA transcriptome landscape of hepatocytes and non-parenchymal cells in healthy and NAFLD mouse liver. *iScience*, **24**, 103233.
32. Postic,C. and Magnuson,M.A. (2000) DNA excision in liver by an albumin-Cre transgene occurs progressively with age. *Genesis*, **26**, 149–150.
33. Qin,Y., Grimm,S.A., Roberts,J.D., Chrysovergis,K. and Wade,P.A. (2020) Alterations in promoter interaction landscape and transcriptional network underlying metabolic adaptation to diet. *Nat. Commun.*, **11**, 962.
34. Miranda,D.A., Krause,W.C., Cazenave-Gassiot,A., Suzawa,M., Escusa,H., Foo,J.C., Shihadih,D.S., Stahl,A., Fitch,M., Nyangau,E. *et al.* (2018) LRH-1 regulates hepatic lipid homeostasis and

maintains arachidonoyl phospholipid pools critical for phospholipid diversity. *JCI Insight*, **3**, e96151.
35. Caputo,L., Witzel,H.R., Kolovos,P., Cheedipudi,S., Looso,M., Mylona,A., van,I.W.F., Laugwitz,K.L., Evans,S.M., Braun,T. *et al.* (2015) The ISL1/LDB1 complex orchestrates genome-wide chromatin organization to instruct differentiation of multipotent cardiac progenitors. *Cell Stem Cell*, **17**, 287–299.
36. Zhang,F., Tanasa,B., Merkurjev,D., Lin,C., Song,X., Li,W., Tan,Y., Liu,Z., Zhang,J., Ohgi,K.A. *et al.* (2015) Enhancer-bound LDB1 regulates a corticotrope promoter-pausing repression program. *Proc. Natl Acad. Sci. U.S.A.*, **112**, 1380–1385.
37. Monahan,K., Horta,A. and Lomvardas,S. (2019) LHX2- and LDB1-mediated *trans* interactions regulate olfactory receptor choice. *Nature*, **565**, 448–453.
38. Shen,Y., Yue,F., McCleary,D.F., Ye,Z., Edsall,L., Kuan,S., Wagner,U., Dixon,J., Lee,L., Lobanenkov,V.V. *et al.* (2012) A map of the *cis*-regulatory sequences in the mouse genome. *Nature*, **488**, 116–120.
39. Alder,O., Cullum,R., Lee,S., Kan,A.C., Wei,W., Yi,Y., Garside,V.C., Bilenky,M., Griffith,M., Morrissy,A.S. *et al.* (2014) Hippo signaling influences HNF4A and FOXA2 enhancer switching during hepatocyte differentiation. *Cell Rep.*, **9**, 261–271.
40. Nakamura,H., Mukai,M., Komatsu,K., Tanaka-Okamoto,M., Itoh,Y., Ishizaki,H., Tatsuta,M., Inoue,M. and Miyoshi,J. (2005) Transforming growth factor-beta1 induces LMO7 while enhancing the invasiveness of rat ascites hepatoma cells. *Cancer Lett.*, **220**, 95–99.
41. Holaska,J.M., Rais-Bahrami,S. and Wilson,K.L. (2006) Lmo7 is an emerin-binding protein that regulates the transcription of emerin and many other muscle-relevant genes. *Hum. Mol. Genet.*, **15**, 3459–3472.
42. Ediger,B.N., Lim,H.W., Juliana,C., Groff,D.N., Williams,L.T., Dominguez,G., Liu,J.H., Taylor,B.L., Walp,E.R., Kameswaran,V. *et al.* (2017) LIM domain-binding 1 maintains the terminally differentiated state of pancreatic beta cells. *J. Clin. Invest.*, **127**, 215–229.
43. Oosterveer,M.H., Mataki,C., Yamamoto,H., Harach,T., Moullan,N., van Dijk,T.H., Ayuso,E., Bosch,F., Postic,C., Groen,A.K. *et al.* (2012) LRH-1-dependent glucose sensing determines intermediary metabolism in liver. *J. Clin. Invest.*, **122**, 2817–2826.
44. Kir,S., Zhang,Y., Gerard,R.D., Kliewer,S.A. and Mangelsdorf,D.J. (2012) Nuclear receptors HNF4α and LRH-1 cooperate in regulating CYP7A1 *in vivo*. *J. Biol. Chem.*, **287**, 41334–41341.
45. Reizel,Y., Morgan,A., Gao,L., Lan,Y., Manduchi,E., Waite,E.L., Wang,A.W., Wells,A. and Kaestner,K.H. (2020) Collapse of the hepatic gene regulatory network in the absence of FoxA factors. *Genes Dev.*, **34**, 1039–1050.
46. Thakur,A., Wong,J.C.H., Wang,E.Y., Lotto,J., Kim,D., Cheng,J.C., Mingay,M., Cullum,R., Moudgil,V., Ahmed,N. *et al.* (2019) Hepatocyte nuclear factor 4-alpha is essential for the active epigenetic state at enhancers in mouse liver. *Hepatology*, **70**, 1360–1376.
47. Kiourtis,C., Wilczynska,A., Nixon,C., Clark,W., May,S. and Bird,T.G. (2021) Specificity and off-target effects of AAV8-TBG viral vectors for the manipulation of hepatocellular gene expression in mice. *Biol. Open*, **10**, bio058678.
48. Lee,S., Zhou,P., Whyte,S. and Shin,S. (2020) Adeno-associated virus serotype 8-mediated genetic labeling of cholangiocytes in the neonatal murine liver. *Pharmaceutics*, **12**, 351.
49. Guillam,M.T., Hummler,E., Schaerer,E., Yeh,J.I., Birnbaum,M.J., Beermann,F., Schmidt,A., Deriaz,N. and Thorens,B. (1997) Early diabetes and abnormal postnatal pancreatic islet development in mice lacking Glut-2. *Nat. Genet.*, **17**, 327–330.
50. Hunter,C.S., Dixit,S., Cohen,T., Ediger,B., Wilcox,C., Ferreira,M., Westphal,H., Stein,R. and May,C.L. (2013) Islet α-, β-, and δ-cell development is controlled by the Ldb1 coregulator, acting primarily with the islet-1 transcription factor. *Diabetes*, **62**, 875–886.
51. Loyd,C., Liu,Y., Kim,T., Holleman,C., Galloway,J., Bethea,M., Ediger,B.N., Swain,T.A., Tang,Y., Stoffers,D.A. *et al.* (2017) LDB1 regulates energy homeostasis during diet-induced obesity. *Endocrinology*, **158**, 1289–1297.
52. Zhang,T.T., Zhang,Z.Q., Dong,Q., Xiong,J. and Zhu,B. (2020) Histone H3K27 acetylation is dispensable for enhancer activity in mouse embryonic stem cells. *Genome Biol.*, **21**, 45.
53. Martire,S., Nguyen,J., Sundaresan,A. and Banaszynski,L.A. (2020) Differential contribution of p300 and CBP to regulatory element acetylation in mESCs. *BMC Mol. Cell Biol.*, **21**, 55.
54. Schuh,A.H., Tipping,A.J., Clark,A.J., Hamlett,I., Guyot,B., Iborra,F.J., Rodriguez,P., Strouboulis,J., Enver,T., Vyas,P. *et al.* (2005) ETO-2 associates with SCL in erythroid cells and megakaryocytes and provides repressor functions in erythropoiesis. *Mol. Cell. Biol.*, **25**, 10235–10250.
55. Goardon,N., Lambert,J.A., Rodriguez,P., Nissaire,P., Herblot,S., Thibault,P., Dumenil,D., Strouboulis,J., Romeo,P.H. and Hoang,T. (2006) ETO2 coordinates cellular proliferation and differentiation during erythropoiesis. *EMBO J.*, **25**, 357–366.
56. Soler,E., Andrieu-Soler,C., de Boer,E., Bryne,J.C., Thongjuea,S., Stadhouders,R., Palstra,R.J., Stevens,M., Kockx,C., van Ijcken,W. *et al.* (2010) The genome-wide dynamics of the binding of Ldb1 complexes during erythroid differentiation. *Genes Dev.*, **24**, 277–289.
57. Fujiwara,T., Lee,H.Y., Sanalkumar,R. and Bresnick,E.H. (2010) Building multifunctionality into a complex containing master regulators of hematopoiesis. *Proc. Natl Acad. Sci. U.S.A.*, **107**, 20429–20434.